Electron Beam Freeform Fabrication in the Space Environment

Robert A. Hafley[1], Karen M. B. Taminger[1], and R. Keith Bird[1]
NASA Langley Research Center, Hampton, VA, 23681

[Abstract] The influence of reduced gravitational forces (in space and on the lunar or Martian surfaces) on manufacturing processes must be understood for effective fabrication and repair of structures and replacement parts during long duration space missions. The electron beam freeform fabrication (EBF^3) process uses an electron beam and wire to fabricate metallic structures. The process efficiencies of the electron beam and the solid wire feedstock make the EBF^3 process attractive for use in-space. This paper will describe the suitability of the EBF^3 process in the space environment and will highlight preliminary testing of the EBF^3 process in a zero-gravity environment.

Nomenclature

g = acceleration of gravity
V = volts
W = watts

I. Introduction

FUTURE long-duration human exploration missions will be challenged by constraints on mass and volume allocations available for spare parts. Addressing this challenge will be critical to the success of these missions. As a result, it is necessary to consider new approaches to spacecraft maintenance and repair that minimize the mass and stowage volume that must be allocated for spares while enhancing mission robustness[1].

Solid freeform fabrication (SFF) is a technology that could be used to support fabrication and repair of large space structures, spacecraft primary structure, and replacement components[2]. Production of replacement components by SFF processes during a mission could reduce or eliminate the need to carry a complete inventory of pre-manufactured spares. Rather, replacement components would be generated as needed from feedstock material. As a result, only the total mass of replacements would need to be estimated instead of a prediction of which specific components might be needed. Attempting to predict which components will fail and require replacement will inherently be an inaccurate process and will result in provisioning numerous components that will never be used (wasted mass) while under-provisioning other components.

SFF processes are layer additive processes that can be used to build near-net shaped parts directly from computer numerically controlled techniques without use of molds or tooling. In direct metal deposition SFF processes, an energy source is used to establish a molten pool on a substrate and metal feedstock is introduced into the molten pool. The substrate is then translated to produce the desired part. Direct metal deposition SFF processes utilizing laser or electron beam energy sources offer the greatest potential for space applications. Although the feedstock material can be introduced as either a powder or wire, the wire form is preferable for in-space application because of operational and safety issues associated with management of metallic powder in a microgravity environment. The inert atmosphere typically required by SFF processes to ensure part quality can be met by using the vacuum of space. For this effort an electron beam was chosen over a laser as the energy source due to the higher energy efficiency and ability to couple with reflective materials, such as aluminum. The basic electron beam freeform fabrication (EBF^3) process is described below.

Manufacturing using SFF processes in the space, lunar or Martian environments presents some challenges compared to manufacturing on Earth. The effects of reduced gravitational forces on the SFF process and the resulting geometry and metallurgical quality of a deposited layer must be better understood. The atmosphere, high vacuum in space and on the lunar surface and approximately 400 Pa pressure (primarily CO_2) on the Martian

---

[1] Materials Research Engineer, Advanced Materials & Processing Branch, MS188A.

surface, may change the process thermodynamics and the final material composition due to fugacity of higher vapor pressure elements in a sustained molten pool in a reduced pressure atmosphere. Furthermore, temperature extremes encountered may affect equipment or part tolerances. This work focused on understanding the effects of microgravity on the EBF^3 process and the resulting deposits.

II. Experimental Details

Electron beam freeform fabrication (EBF^3) was selected as a viable candidate for fabricating components in space due to the high energy efficiency of the electron beam and ease of handling and high capture efficiency of the solid wire feedstock. A portable, flight-weight EBF^3 system was built and a series of deposition trials were conducted in microgravity flight tests. These deposition trials were repeated in 1-g for comparison between reduced gravity and Earth's gravity. Heights and widths of the deposition features were measured prior to sectioning the panels for microstructural analysis.

A. Electron Beam Freeform Fabrication Process

The electron beam freeform fabrication (EBF^3) process is a layer additive process that uses computer numerically controlled techniques to build metallic near-net shaped parts. EBF^3 is a direct metal deposition process in which metallic feedstock, typically in the form of wire, is fed into a molten pool that is created by an electron beam focused on a substrate. The electron beam and wire feeder are translated with respect to the substrate to build up a part. The resulting parts are fully dense and produced directly from computer aided design files without molds or tooling. The electron beam can also be used to perform secondary processing, such as surface melting or hole drilling. The production of the electron beam and coupling of the electron beam with the feedstock material make the EBF^3 process highly energy efficient. Virtually 100% of the feedstock material is captured in the finished deposit. The EBF^3 process is capable of rapidly processing all weldable alloys, including highly reflective materials such as aluminum and copper. With the use of multiple wire feeders, functionally graded parts can be produced[3].

B. Portable Electron Beam Freeform Fabrication System

A flight-weight EBF^3 system, Fig. 1, was developed at NASA Langley Research Center to enable the evaluation of microgravity effects on the EBF^3 process using NASA's C-9 Microgravity Research Aircraft. The flight-weight EBF^3 system was designed to meet the safety, size and power requirements of the aircraft. The system comprises a fixed electron beam gun, wire feeder, four-axis positioning system, vacuum system, and associated controls and power supplies. The major subsystems, including the vacuum chamber, vacuum pumps, electron beam gun, wire feeder, and positioning system, were produced under contract and integrated at Langley. The vacuum chamber is a 900 mm cube, constructed of aluminum. The chamber walls provide adequate radiation shielding for the

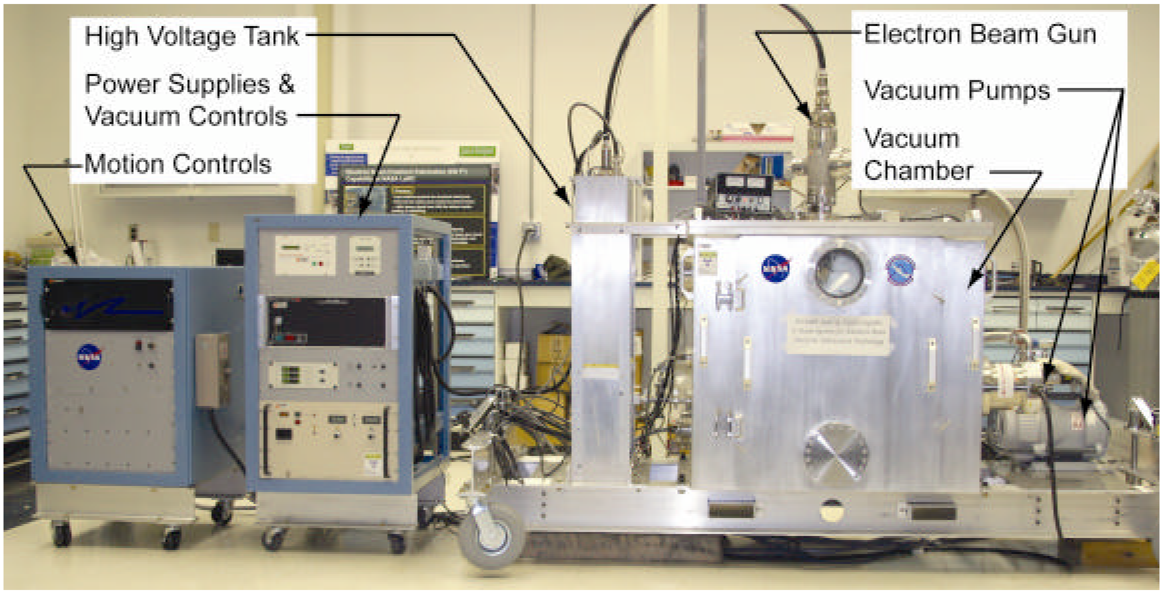

Figure 1. Flight-weight electron beam freeform fabrication (EBF^3) system.

accelerating voltages used. The vacuum pumping system is comprised of a dry scroll mechanical pump and a turbomolecular pump with magnetically levitated bearings. The pumps are capable of achieving a pressure of 10^{-4} Pa in the vacuum chamber. The flight-weight EBF^3 system is operated from a laptop computer using control software developed in-house.

The interior of the vacuum chamber is shown in Fig. 2. The electron beam gun is inserted through the top of the chamber. The electron beam gun is air-cooled and designed to provide 3-5 kW of beam power with an accelerating voltage in the range of 10-30 kV. A lanthanum hexaboride (LaB_6) cathode was chosen to provide a longer operating life compared to a refractory metal cathode. The wire feeder is attached to the electron beam gun and feeds wire in the +Y direction. The wire feeder is capable of feeding wire up to 1 mm diameter from standard 100 mm diameter welding wire spools at speeds up to 100 mm s^{-1}. The positioning system is attached to the floor of the vacuum chamber and provides motion to the substrate relative to the stationary electron beam gun and wire feeder. The positioning system consists of three orthogonal linear axes which provide a range of motion of 300 mm in X and Y and 150 mm in Z at speeds up to 40 mm s^{-1} and a rotary axis which provides 360° of rotation. Naming conventions for the axes are shown relative to the substrate in Fig. 2.

C. Microgravity Flight Tests

Tests were conducted aboard NASA's C-9 Microgravity Research Aircraft to determine the effects of microgravity on the EBF^3 process. The C-9 is flown in a series of parabolic trajectories in order to generate microgravity, Fig. 3. The duration of microgravity is approximately 15-20 seconds followed by a 45-second long 1.8-g pullout. A flight day typically consists of 40 parabolas, flown in sets of 10, with a 5-minute break between sets. Eleven days of flight tests were conducted. Since the parabolas were flown in rapid succession, each flight plate was planned to include numerous experiments because there was insufficient time to change plates and pump back down to the operating pressure during the flight. Deposits were only conducted during the 0-g portions of the flight trajectory, which limited the size and height of the components that could be built.

The objectives for the flight testing were as follows: demonstrate that the EBF^3 process works in 0-g; conduct deposition trials with a range of translation speeds and wire feed rates to explore the process window in 0-g; explore control issues for direction of wire entry into the molten pool; examine the effects of gravity on the EBF^3 process; determine the effects of depositing a taller build, including resuming deposition after prolonged interruption. For comparison purposes, a duplicate of each flight test plate was prepared on the ground (in 1-g), using the same timings between deposits as occurred on the aircraft.

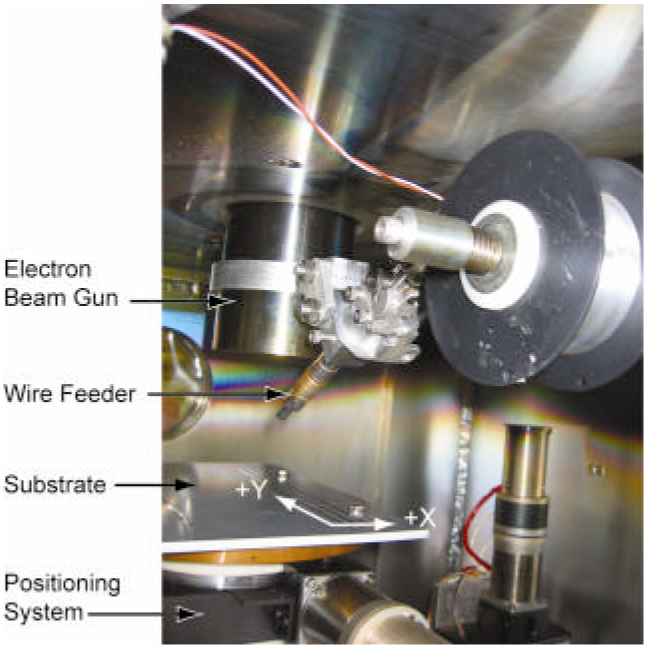

Figure 2. Interior of portable EBF^3 system showing major components and translation conventions.

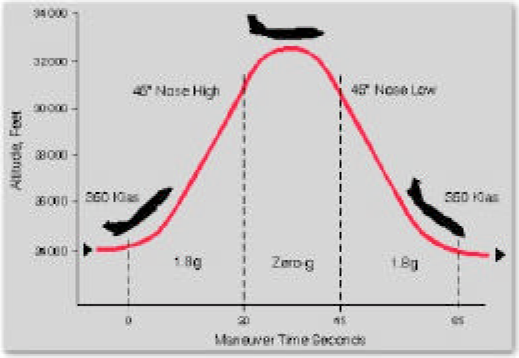

Figure 3. Trajectory flown by NASA's C-9 Microgravity Research Aircraft.

D. Materials and Processing Details

All deposits were made using 0.8 mm diameter aluminum alloy 2319 (Al2319) wire onto 6.35 mm thick aluminum alloy 2219 (Al2219) substrates, which resulted in deposits within the Al2219 composition range (Al-6 wt% Cu, with other trace elements that differentiate between the Al2219 and Al2319 designations). This alloy was selected because it is readily weldable and commonly used in space structures such as the International Space Station. Due to the limited number of experiments that could be conducted during the 0-g flight tests, the initial EBF^3 parameters (beam power, translation speed, and wire feed rate) were selected to be well within the typical operational range for Al2219[4]. The wire feed rate and translation speed and direction were systematically varied to achieve the test objectives outlined in the microgravity flight tests section above.

E. Post-Deposition Analysis

After conducting EBF^3 deposition trials during a series of 0-g flight tests and corresponding 1-g ground-based tests, macroscopic photographs were taken to document the condition of each plate. The height and width of each deposit was measured every 12.5 mm along the length of the deposit to record the differences between features and between plates fabricated in 0-g as compared to 1-g. The heights were measured using a digital indicator and the widths were measured using vernier calipers. Afterwards, 45 deposits from each of the 0-g and 1-g plates were cross-sectioned perpendicular to the length of the deposit, mounted, polished and chemically etched. These samples were examined using optical microscopy to identify any changes in the microstructure or porosity that might have occurred during the deposition under different processing conditions at 0-g and 1-g.

III. Results

Key issues associated with the production of components during space missions center on the potential effects of a microgravity environment on the EBF^3 process. In the microgravity environment, body forces on the molten region of the deposited bead become insignificant and surface tension and wetting forces will dominate. Therefore, the cross-sectional shape of the molten region may be different during microgravity deposition than during deposition in a 1-g environment. This will have at least two potentially significant effects. First, the bead cross-section will govern the topography of the exposed surfaces of the final part. The resulting surface condition and associated stress concentrations may affect the mechanical properties of the component. Second, closed-loop process control schemes may rely on monitoring the shape of the molten portion of the deposited bead. Since the bead shape in microgravity may be somewhat different from that in a 1-g environment, it is essential that the nominal shape in microgravity be fully characterized.

Initial trials reveal that the process works well in 0-g if the correct distance between the wire and the substrate is maintained, Fig. 4. If this distance is too great in 1-g, small droplets form and fall to the substrate as the gravitational forces exceed the surface tension. In 0-g molten spheres form at the end of the wire and expand as wire continues to feed and melt in the electron beam, Fig. 5. If the spheres come in contact with the deposit, wetting forces wick the molten sphere to the deposit attaching it to the surface. This results in an uneven deposit height that is exacerbated with each additional layer. Vibrations in the equipment have also induced separation of the spheres from the wire before they attach to the deposit or substrate, resulting in molten droplets floating loose inside the vacuum chamber.

Testing in 0-g showed that maintaining the correct distance between the wire and substrate is more important in 0-g than in 1-g. The system was operated in an open loop mode so that the heights were manually programmed prior to initiating the tests. During the flights the distance between the wire and the substrate was controlled manually by the operator. A closed loop control system is under development to incorporate a feedback loop that automatically maintains the correct distance between the wire and the substrate.

Figures 6 and 7 show plates that were built in 0-g and 1-g, respectively. These particular plates contain 23 different elements to evaluate the effect of wire feed rate and deposition direction. Four multiple layer deposits were produced; the remainder were each one layer high. The end point of each deposit consists of a characteristic accumulation of excess material as noted in Fig. 6. This excess material is a result of non-optimized termination sequencing of translation, wire feed and electron beam. These features are useful reference points to determine the direction of travel for the different elements deposited on the plate. The wire feed rates for the single layer deposits in the X and Y directions varied by a factor of three from lowest to highest, while the multiple layer and circular deposits were performed at the highest of the three wire feed rates. There was no visual difference observed between the deposits produced in 0-g and those produced in 1-g.

Prior experience in 1-g and standard practice in welding processes that use an auxiliary wire feed has shown that it is preferable to have the wire enter the leading edge of the molten pool (-Y direction)[5]. Wire entry from other than

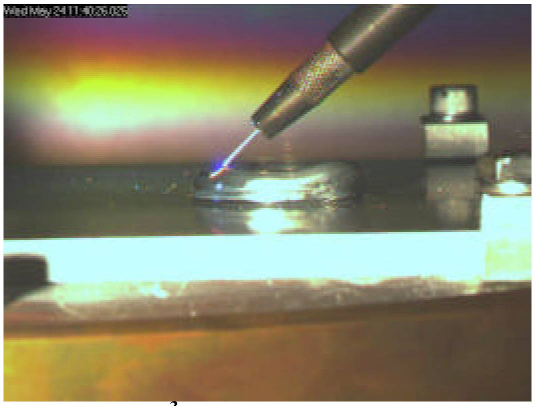

Figure 4. EBF^3 deposit made in 0-g with correct distance between wire feeder and substrate.

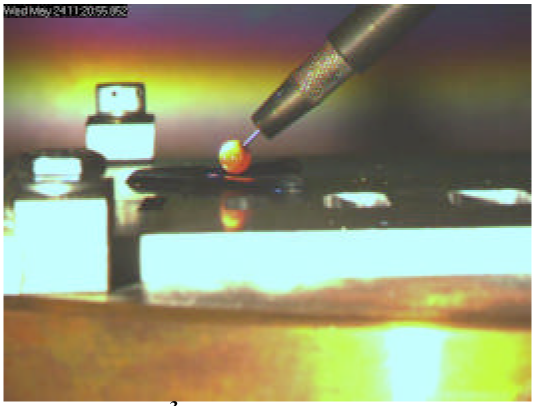

Figure 5. EBF^3 deposit made in 0-g with incorrect distance between wire feeder and substrate.

the leading edge has been observed to slightly alter the geometry of the deposit by pushing the deposit in the direction that the wire is feeding. However, the ability to feed wire into the molten pool from any angle greatly simplifies the path planning for the fabrication process and potentially reduces the number of axes of motion required for the process. Tests were conducted to determine if there is a difference in the response of the molten pool to the effects of surface tension or wetting forces in a microgravity environment as a result of differing wire feed directions into the molten pool. The average (measured in 3 places along the deposit) and the range of heights of four selected deposits produced at 1-g and 0-g are shown in Fig. 8. These deposits were produced with the same wire feed rate, translation speed, and beam power and represent four wire entry directions: 1) leading the molten pool and parallel to the direction of travel; 2) trailing the molten pool and parallel to the direction of travel; 3) feeding into the side of the molten pool and perpendicular to the direction of travel in a positive direction; and 4) feeding into the side of the molten pool and perpendicular to the direction of travel in a negative direction. The heights of deposits produced in 1-g were more uniform than those produced in 0-g, regardless of which direction the wire enters the molten pool. Within the precision of these measurements no clear trend in deposit height was noted as a function of gravity or wire entry direction. Further detailed analysis is required to ascertain if the deposit height variations measured is significant.

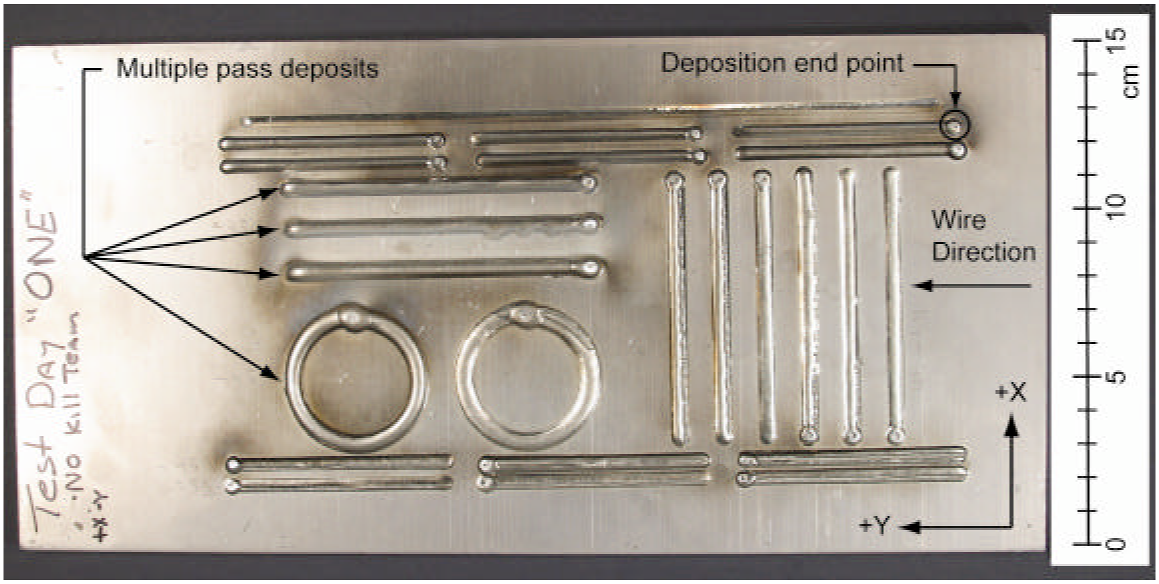

Figure 6. EBF^3 deposits conducted in 0-g to evaluate the effect of wire feed rate and direction in microgravity.

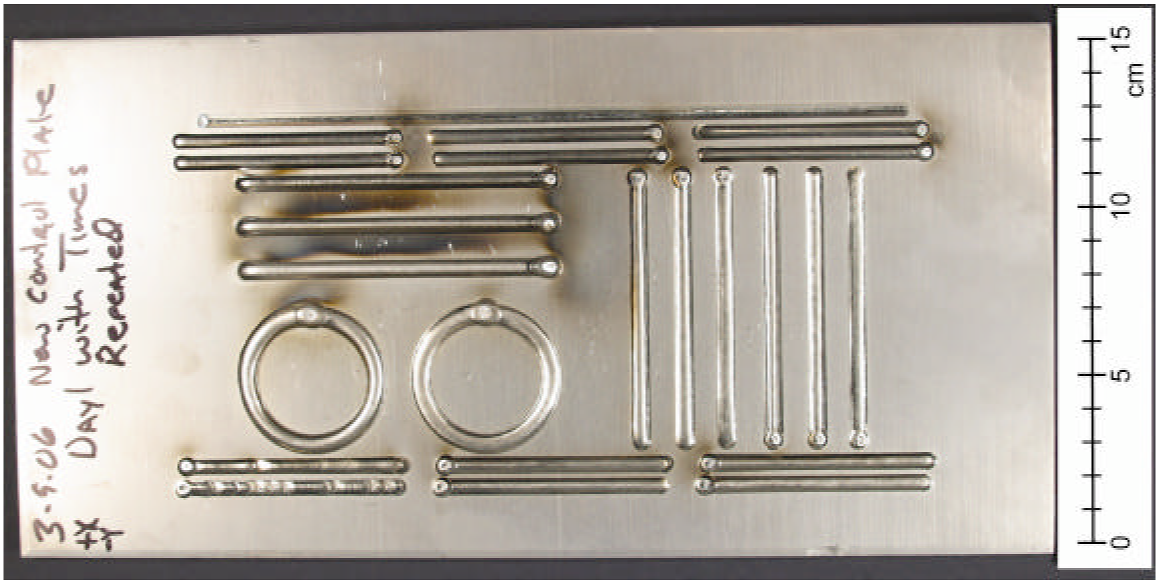

Figure 7. $\mathbf{EBF^3}$ deposits conducted in 1-g to compare to similar plate produced in 0-g (shown in Fig. 6).

To explore the effects of gravity on the EBF^3 process, advantage was taken of the high-g portion of the flight to exaggerate the influence of gravity. A deposit was initiated during the 0-g portion of the parabola and continued through a 2-g pullout. The height of the deposit was measured along the length and correlated with the acceleration, which was measured with an accelerometer mounted in the control cabinet just aft of the vacuum chamber. There appears to be a slight decrease in deposit height with increasing gravity, Fig. 9, but not a significant difference. The variations seen in deposit height are partially attributed to aircraft vibrations transferred to the deposition region through the equipment (the equipment is bolted to the frame of the aircraft for safety).

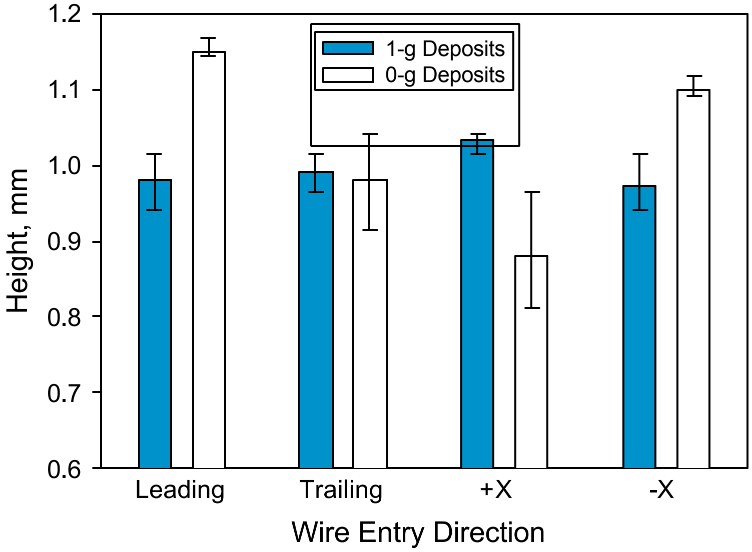

Figure 8. Comparison of deposit height in 1-g versus 0-g for four wire entry directions.

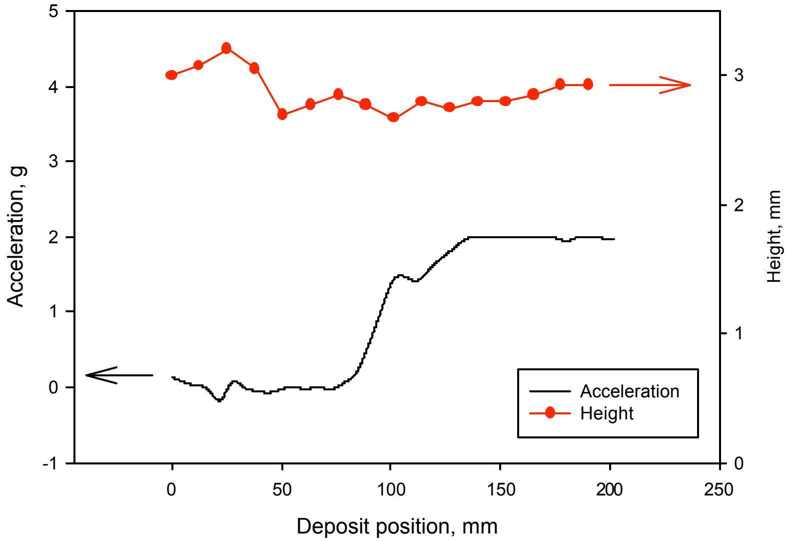

Figure 9. Deposit height versus acceleration for deposit spanning 0-g to 2-g.

Optical micrographs of the cross-sections of single layer deposits taken from the same location and produced with the same parameters in 0-g and 1-g are shown in Figs. 10 and 11. This is a typical microstructure observed in EBF^3 deposits [6]. Both deposits exhibit typical cast aluminum solidification microstructure, consisting of columnar grains initiating at the bottom of the molten pool and growing perpendicular to the substrate surface . The light gray area in the substrate below the deposit is the heat affected zone (HAZ), an area where elevated temperature, insufficient for melting, has caused a change in the substrate microstructure. The deposits exhibit similar cross-sectional profiles. Porosity is a significant documented problem occurring in processing molten materials in 0-g[7]. However, there was no evidence of porosity in deposits produced in 0-g, based upon examination of 45 cross-sections produced in 0-g.

Previous work has shown that for thin wall deposits less than five layers high, cooling is dominated by a broad path through the substrate[8]. For higher deposits, cooling is restricted to the path through the previous layers, resulting in lower cooling rates and higher temperatures in the molten pool. As surface tension and wetting forces are both temperature dependent this may become an issue for larger builds. This is difficult to evaluate aboard the C-9 due to the limited time in 0-g (15-20 s). It was also desired to resume an interrupted part to determine if there were any significant difficulties or flaws created at the interrupted layer. Therefore, in order to produce a tall deposit in 0-

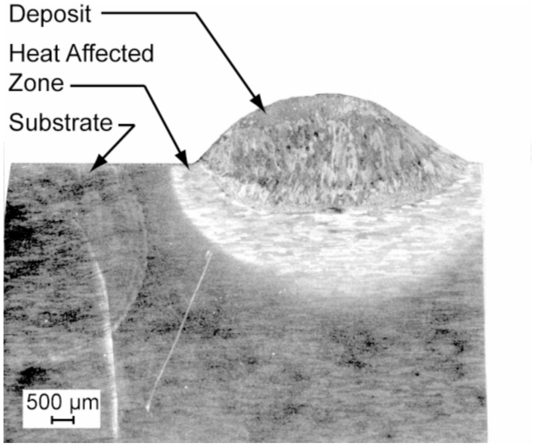

Figure 10. Microstructure of single layer EBF^3 deposit produced in 0-g.

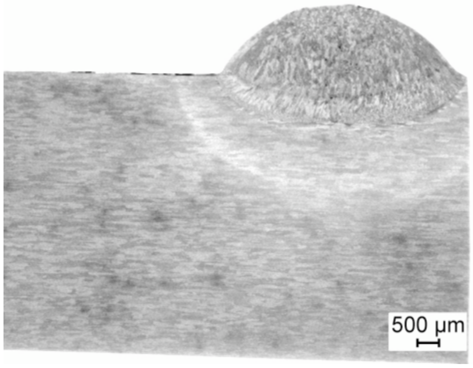

Figure 11. Microstructure of single layer EBF^3 deposit produced in 1-g.

g a 70 mm diameter cylindrical build was conducted for two consecutive flights. On the first flight 21 layers were deposited resulting in a cylinder approximately 14 mm tall. All axes of the positioning system were then returned to the home position and all systems were powered down. After approximately four hours, all systems were powered up, the positioning system was returned to the last deposition location and the build was resumed on the second flight. An additional 27 layers were successfully deposited in 0-g, resulting in a cylinder approximately 30 mm tall, Fig. 12. No difficulties were encountered during the deposition. The cylinder is somewhat wider at the top than at the base, indicating a spread of the molten pool. This spread is due to the increased temperature experienced as the build progressed, caused by the lower cooling rate resulting from the restricted cooling path through the deposit. This increase in the width of the deposit has also been documented in 1-g[4].

Figure 12. 30 mm tall cylinder built over two flights.

Several equipment issues were identified during flight testing. The magnetically levitated bearings of the turbomolecular pump were not capable of withstanding the vibrational and gyroscopic loads imposed during flight testing. A switch to a turbomolecular pump with ceramic bearings and a change in pump orientation to minimize gyroscopic loads appears to have corrected this issue. Some difficulties were encountered with the wire feeder jamming if the wire contacted a surface prior to melting. The wire feeder was redesigned to provide a simplified wire path. This appears to have eliminated jamming of the wire feeder. These modifications have increased the robustness of the existing flight-weight EBF^3 system. They have also been incorporated into the designs for a next-generation system to enable more reliable hardware operations.

IV. Summary

The EBF^3 process has been demonstrated to work in 0-g, as long as the distance between the substrate and the wire feeder is carefully maintained. It was possible to produce deposits using several different translation speeds and wire feed rates in a microgravity environment. Furthermore, EBF^3 deposits were successfully produced in 0-g with wire entering the molten pool from any direction relative to the translation direction. These demonstrations support the concept of developing a simple EBF^3 system to fabricate near-net shaped components in a microgravity environment to support long duration human exploration missions in space. Within the limited parameter space examined using Al2319, no significant difference in deposit height or microstructure was observed between deposits produced in 0-g and 1-g. The single deposit produced under 2-g appears to be slightly shorter than the deposits produced in 0-g and 1-g, but not significantly different. This is important because testing in 0-g is difficult, costly, and has severe limitations due to the short duration in 0-g and vibrations introduced through the airframe. Since the EBF^3 process has been demonstrated to work in 0-g and produce deposits comparable to those produced in 1-g, laboratory testing can be expected to reasonably approximate results in 0-g, allowing process development and certification to be conducted in ground based tests.

Equipment issues identified during flight testing have been incorporated into future designs for increased robustness and reliability. Future plans include modeling for improved understanding of the process and development of a closed loop control system and a next generation EBF^3 system that will be closer to a space flight configuration.

References

[1] Watson, K., D. Petersen, and R. Crockett, "Application of Solid Freeform Fabrication Technology to NASA Exploration Missions," *Proceedings, 10th Solid Freeform Fabrication Symposium*, Austin, TX: University of Texas at Austin, 1999, pp. 857 – 864.

[2] Taminger, K. M. B., R. A. Hafley, and D. L. Dicus, "Solid Freeform Fabrication: An Enabling Technology for Future Space Missions," *Proceedings, 2002 International Conference on Metal Powder Deposition for Rapid Manufacturing*, San Antonio, TX: Metal Powder Industries Federation, 2002, pp. 51-60.

[3] Domack, M. S., R. A. Hafley, K. M. B. Taminger, "Characterization of Aluminum and Aluminum-Lithium Graded Composition Material Produced by Electron Beam Freeform Fabrication", presented at *Solid Freeform Fabrication Symposium*, Austin, TX: University of Texas at Austin, 2004.

[4] Taminger, K. M. B., and R. A. Hafley, "Characterization Of 2219 Aluminum Produced By Electron Beam Freeform Fabrication", *Proceedings, 13th Solid Freeform Fabrication Symposium*, Austin, TX: University of Texas at Austin, 2002, pp. 482-489.

[5] O'Brien, A. (ed.), *Welding Handbook Volume 2*,9th ed., American Welding Society, Miami, 2004, Chaps. 3, 7.

[6] Domack, Marcia S,. Karen M. B. Taminger, and Matthew Begley, "Metallurgical Mechanisms Controlling Mechanical Properties of Aluminum Alloy 2219 Produced By Electron Beam Freeform Fabrication," *Materials Science Forum* Vols. 519-521, 2006, pp. 1291-1296.

[7] Pettegrew, Richard D., Peter M. Struk, John K. Watson, Daniel R. Haylett, "Experimental Methods in Reduced-Gravity Soldering Research," NASA/TM—2002-211993, 2002.

[8] Taminger, Karen M., Robert A. Hafley, and Marcia S. Domack, "Evolution and Control of 2219 Aluminum Microstructural Features through Electron Beam Freeform Fabrication," *Materials Science Forum* Vols. 519-521, 2006, pp. 1297-1302.